

# Monitoring changes in the viscoelastic properties of thin polymer films by the quartz crystal resonator

Jong-Min Kim<sup>a,\*</sup>, Sang-Mok Chang<sup>a</sup>, Hiroshi Muramatsu<sup>b</sup>

<sup>a</sup>Department of Chemical Engineering, Dong-A University, 840 Hadan-dong, Pusan 604-714, South Korea

<sup>b</sup>Advanced Technology Center, Seiko Instruments Inc., Matsudo-shi, Chiba 271, Japan

Received 20 October 1997; received in revised form 7 April 1998; accepted 7 July 1998

## Abstract

This paper shows that a quartz crystal resonator is applicable to the investigation of rheological property changes of polymer blend and polymer films by the simultaneous measurement of resonant frequency and resonant resistance of the quartz crystal resonator. Phase transition phenomena of PMMA/PVAc blend films were studied in the thermal cycles. Viscoelastic property changes of PMMA homopolymers including a certain amount of plasticizer and the dependence of molecular size in blend film on phase transition temperature were also investigated. Both the resonant frequency and resonant resistance of film coated quartz crystals changed critically at the glass transition temperature. The responses of the resonant resistance showed more clear change than those of the resonant frequency because the resonant resistance directly reflects the information of energy dissipation in the coated films. The responses in the thermal cycle were represented as diagrams of the resonant frequency versus the resonant resistance and  $dR/dF$  versus temperature for detailed explanations. These diagrams showed clear glass transition temperatures of the films in the thermal cycles. © 1999 Elsevier Science Ltd. All rights reserved.

**Keywords:** Microrheology; Phase (glass) transition; QCA(QCR)

## 1. Introduction

A well-known analytical tool, quartz crystal microbalance (QCM), was first introduced by Sauerbrey [1] with his famous equation that could convert frequency shift of the quartz crystal to the mass change of electrode surface. The general formula is shown as follows:

$$\Delta F = \Delta m F^2 / (\mu \rho_Q)^{1/2} \quad (1)$$

where  $\Delta F$  is the resonant frequency shift of quartz crystal,  $F$  is the resonant frequency of quartz crystal,  $\Delta m$  is the surface mass change,  $\mu$  is the shear modulus of quartz crystal,  $\rho_Q$  is the density of quartz crystal and  $A$  is the surface area of the quartz crystal. Although the assumptions of both forming an elastic film and no radial influence of the sensitivity on the electrode are necessary to use this equation, it is believed as a suitable equation to treat frequency data of the quartz crystal resonator (QCR) in the air.

In the beginning of the 1980s, it has been reported that QCR is applicable in contact with liquid [2], and the frequency equation of quartz crystal has been derived by

Kanazawa et al. [3] as follows;

$$\Delta F = -F^{3/2} (\rho_L \eta / \pi \mu \rho_Q)^{1/2} \quad (2)$$

where  $\eta$  is the viscosity of the contacted liquid and  $\rho_L$  is the density of the contacted liquid. In this equation, it is understandable that the resonant frequency change of quartz crystal includes the information of mass change and viscoelastic change of its contacted environment. Eqs. (1) and (2) were applied on the several important applications such as electrochemical mass detecting sensor [4], immunoassays [5–7] and monitoring liquid viscosity [8] using the resonant frequency of the quartz crystal.

In 1988, one of the authors successfully derived the equation describing a relationship of resonant resistance and resonant frequency for the quartz crystal in contact with liquid by combining the electrical equivalent circuit and mechanical model [9] as follows;

$$R_1 = (2\pi F \rho_L \eta)^{1/2} A / k^2 \quad (3)$$

where  $k$  is the electro-mechano coupling factor.

This equation indicates that the resonant resistance is

\* Corresponding author.

influenced by the density and viscosity of contacted liquid as well as the resonant frequency.

In most applications of quartz crystal, it is important to know the rigidity of coated films on the electrode because only elastic films show a linear relation between the surface mass change and the resonant frequency change. Our group reported a rough method that could estimate the change in viscoelasticity by measuring the resonant frequency and the resonant resistance simultaneously [11,13] with an apparatus (QCA917, Seiko EG & G). In those papers, we denoted QCM as QCA (quartz crystal analyzer) because its measuring variables were not only the frequency change but also the impedance of the quartz crystal. Using this apparatus, we can estimate the rigidity factor of a film by comparing the values of resonant frequency and resonant resistance [10–12], however, we still do not know the exact ratios of the resonant resistance and resonant frequency that indicate the film is rigid enough to give the linear relation between the resonant frequency change and the mass change.

The phase transition phenomena of polymers have been continuously of interest to polymer scientists because they provide both commercial usability and basic properties. Especially in blend films, the detection of phase transition temperature is one of the spotting themes because the phase transition temperature is used as a criterion of blend miscibility [14–16]. There are several instruments for detecting these phenomena based on the thermal analytical methods such as DSC (differential scanning

calorimetry), DTA (differential thermal analysis), TOA (thermal optical analysis), TMS (probe penetration thermomechanical analysis), GPC (gel permeation chromatography) and light scattering method. However, these methods have a problem in detecting small amounts of sample and are short of information for describing the dynamic rheology changes.

In this paper, we show the suitability of the QCR in detection of the rheological property changes using PMMA (poly methyl methacrylate)/PVAc (poly vinyl acetate) blend film and PMMA homopolymer including a certain amount of a plasticizer.

## 2. Method

### 2.1. Materials

Two types of PMMA (1.  $M_w = 90\,000$ , 2.  $M_w = 15\,000$ ) and PVAc ( $M_w = 110\,000$ ) were purchased from Aldrich Chemical Co. Both polymers were characterized by GPC and DSC measurement. PMMA of the higher molecular weight was used for preparing blend solution and that of the lower molecular weight was used for making homopolymer solution including a plasticizer. Di-*n*-butyl phthalate ( $C_6H_4(COOC_4H_9)_2$ ) and ethyl acetate ( $CH_3COOC_2H_5$ ) were purchased from Wako Pure Chemical Co. and used as received. Deionized-distilled

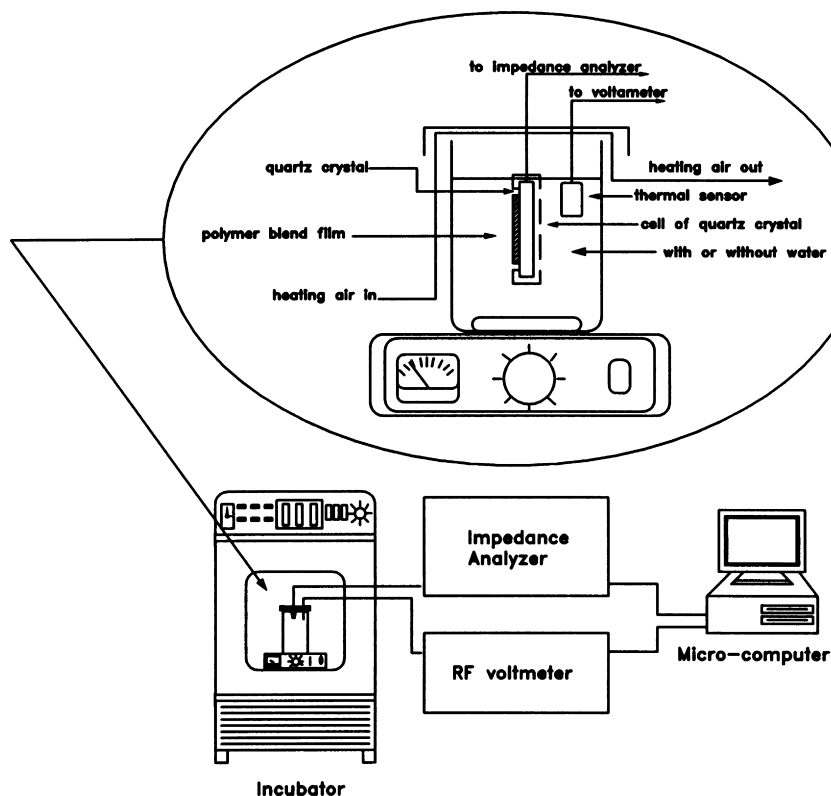


Fig. 1. Schematic diagram of experimental system.

water with ion conductivity under  $0.1 \mu\text{S}/\text{cm}$  was also used for detecting the rheological property changes of the polymer-coated quartz crystal immersed in water during a thermal cycle.

2.2. Instruments and apparatus

A 9-MHz AT-cut quartz crystal (dimension:  $8 \times 8 \times 0.18 \text{ mm}$ ) was prepared by forming gold electrode (thickness about 2500 nm) on both sides of quartz crystals by a sputtering method with Ti underlayers (thickness about 5 nm).

A schematic diagram of the measuring system is shown in Fig. 1. An impedance analyzer (Yokogawa Hewlett Packard, model 4192A) is used for the simultaneous measurements of the resonant frequency and resonant resistance. An incubator (Advantec, model PE-314) is used for temperature sweep. The temperature accuracy of this incubator was shown ( $\pm 0.2^\circ\text{C}$  for the sweep rate of  $0.8^\circ\text{C}/\text{min}$ ). A Pt thin layer thermal sensor and a voltammeter (Advantest, model TR6840) are used for storing the measured data. Polymer film-coated quartz crystal is located in a Teflon cell, which is similar to an electrochemical cell of the quartz crystal. All the experiments were controlled by a personal computer (Epson, model PC-286LS) via a GPIB

interface. A DSC (Perkin-Elmer DSC7) was also used for comparing the results obtained by the QCR method with its own.

2.3. Evaluations of the resonant condition and casting quantity

As described in a previous paper [9], the resonant frequency and resonant resistance are determined by the admittance measurement of a quartz crystal in the electrical equivalent circuit. The admittance of quartz crystal is expressed as follows:

$$Y = 1/(R_1 + j\omega L_1 + 1/j\omega C_1) + j\omega C_0 \tag{4}$$

Eq. (4) is convertible using conductance ( $G$ ) and susceptance ( $B$ ) as follows:

$$(G - 1/(2R_1))^2 + (B - \omega C_0)^2 = (1/(2R_1))^2 \tag{5}$$

The resonant resistance is obtained as the reciprocal expression of the maximum conductance value as depicted in Fig. 2.

Fig. 2(a) and (b) are the admittance diagrams for a bare quartz crystal, Fig. 2(c) and (d) are the admittance diagrams that cast about  $30 \mu\text{l}$  of PMMA/PVAc solution on the quartz crystal with 50/50 blend ratio.

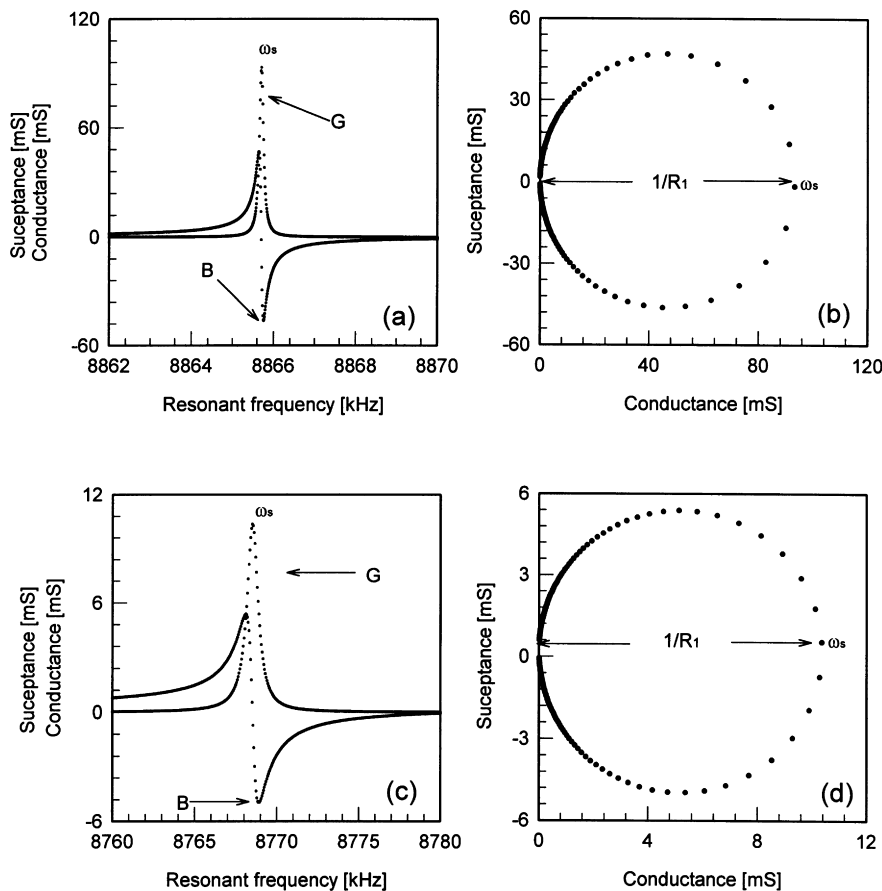


Fig. 2. Admittance diagrams of a quartz crystal with gold electrodes (a, b) and  $30 \mu\text{l}$  of PMMA/PVAc (50/50) blend solution cast on a side of a gold electrode (c, d).

About 500 measurements of admittance ( $G$  and  $B$ ) were performed by the stepped frequencies of 25 Hz in the resonant ranges. The radius of circles on the admittance diagrams in Fig. 2(b) and (d) were determined by adopting the data in Eq. (5). The least square method was applied for these calculations. The resonant frequency was determined from the maximum conductance point on the admittance diagram. About 10 points around these maximum points were inserted in a polynomial equation, and the frequency value of this maximum was determined from the equation. In this measuring system, the frequency range was set up automatically using a resonant frequency value previous to the center frequency of the next measuring frequency range. The average measurement interval was about 30 s at the continuous measurement. The reproducibility of this resonant frequency measurement was within 1 Hz for the quartz crystal in the air and 10 Hz for the quartz crystal immersed in water at 30°C.

Comparing Fig. 2(a) and (c), it is clear that the resonant frequency and conductance are changed by the cast of film. The  $Q$  factor of a quartz crystal is defined as the ratio of the energy stored to the energy lost during oscillation and is nearly equivalent to the inverse of energy dissipation during oscillation [17–19]. The  $Q$  factors of the two quartz crystals are also calculated by applying the following equation:

$$Q = \omega_s / (\omega_2 - \omega_1) \approx \omega_{G \max} / (\omega_2 - \omega_1) \text{ additionally } \omega_s \\ = \sqrt{1/LC}, \text{ i.e. } Q = \frac{1}{R} \sqrt{\frac{L}{C}}$$

where  $L$  is inductance,  $C$  is serial capacitance,  $R$  is the resonant resistance,  $\omega_s$  is the frequency giving the maximum value of conductance  $G$ ,  $\omega_1$  and  $\omega_2$  are the frequencies at the maximum and minimum values of susceptance  $B$ .

The observed values of the  $Q$  factor are 120 000 for the bare quartz crystal with gold electrode and 15 000 for the PMMA/PVAc (50/50, 30  $\mu$ l) blend film cast quartz crystal, respectively. The resonant resistance is increased from 8  $\Omega$  of the bare quartz crystal to 78  $\Omega$  of the blend film-cast quartz crystal for the change of the resonant frequency about 30 000 Hz. The ratio of the change in the resonant frequency and resonant resistance is about 0.003  $\Omega$ /Hz, which indicates the film is not perfectly elastic but in the applicable range of Eq. (1) [18].

#### 2.4. The detections of microrheological property change

PMMA/PVAc blend solutions with various blend ratios were prepared as 3 wt% polymers in ethyl acetate. The concentration of added plasticizer in homopolymer solution (3 wt% of PMMA solution) was from 2.5 to 6.3 wt% when its influence to the phase transition temperature was examined. The polymer solutions were cast about 10  $\mu$ l on a side of quartz crystal, and the film coated quartz crystals were located in a room temperature dry chamber for 3 days to get solid films. Typical film thickness studied by AFM

(Seiko Inst. Inc., SPI 3700, constant force mode) measurement showed 500 nm and surface roughness of the films showed near  $\pm 200$  nm. The thermal cyclic experiment was performed by temperature sweep rate of 0.8°C/min in contact with air or water. The same sweep rate was used in DSC measurement.

### 3. Results and discussion

#### 3.1. Detection of phase transitions for PMMA/PVAc blend films

Fig. 3 shows the responses of resonant frequency (a) and resonant resistance (b) of a 50/50 wt% (PMMA/PVAc) cast quartz crystal in a thermal cycle. The weight of the cast film was roughly estimated to 10  $\mu$ g from the direct calculation

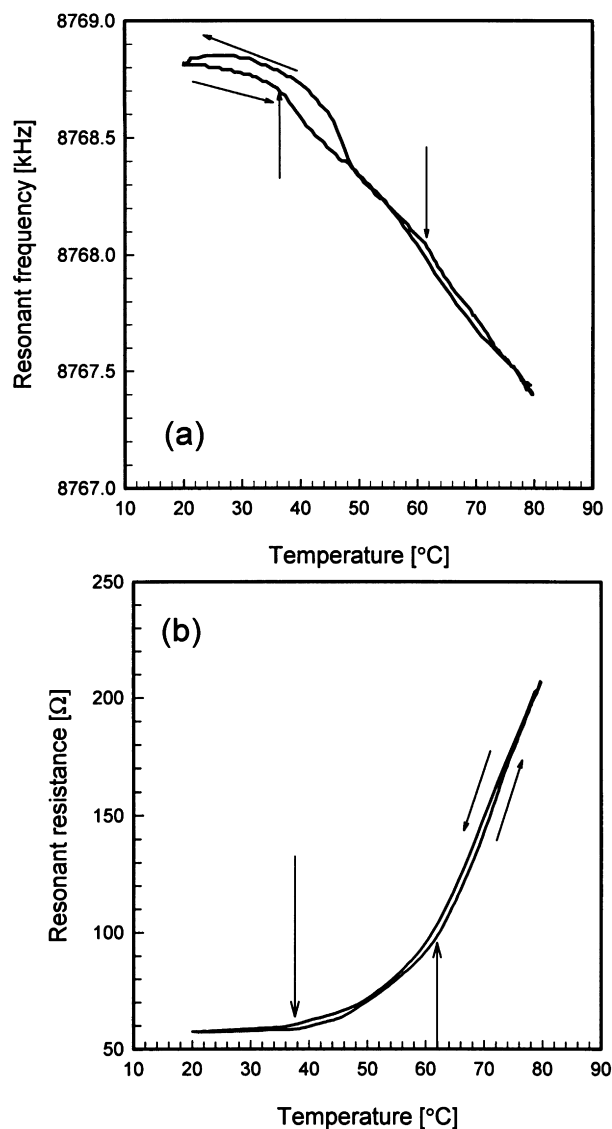


Fig. 3. The resonant frequency (a) and resonant resistance (b) responses of the PMMA/PVAc (50/50) blend film-coated quartz crystal during a thermal cycle.

of the frequency difference between the bare quartz crystal and dried-film-coated quartz crystal. Total data for this sample on progressing the continuous thermal cycles are presented in a previous communication [20]. In this paper, we use the results of the second heating and cooling run by the results of that report.

As described above, we can detect that the microrheological property changes occurred on the surface of quartz crystals by measuring the resonant frequency and resonant resistance, simultaneously. As shown in Fig. 3, the resonant responses for the (50/50) wt% PMMA/PVAc blend film-coated quartz crystal show a good reproducibility meaning no interference effects, such as, surface evaporation of solvent, rearrangement of film structure and other outside influences during the thermal sweeps. In these results, the resonant frequency decreases with increasing temperature, and nearly three different slopes exist with boundaries at about 36 and 63°C. The result of the resonant frequency in the thermal cycle may not coincide with Eq. (1) because the assumption of elastic film coating on the quartz crystal is not perfectly held at the temperature over the phase transition point. Therefore, the changes of resonant frequency do not directly mean a change of surface mass. We have explained these phenomena in a previous paper by the vibration models of quartz crystals combined with different viscoelastic film coatings in contact with different viscoelastic liquids [21]. To investigate this effect, the resonant resistance was measured, as shown in Fig. 3(b). In Fig. 3(b), the resonant resistance is gradually increasing by increasing temperature with two inflection points close to 38 and 62°C in the examined temperature range. These inflection points are understood to be phase transition points. The result of Fig. 3(b) indicates that two-phase transition temperatures of the blend film exist in the measured temperature range, and the increasing slopes of resonant resistance are different in the boundaries of these two temperatures. These results also show that the response of the

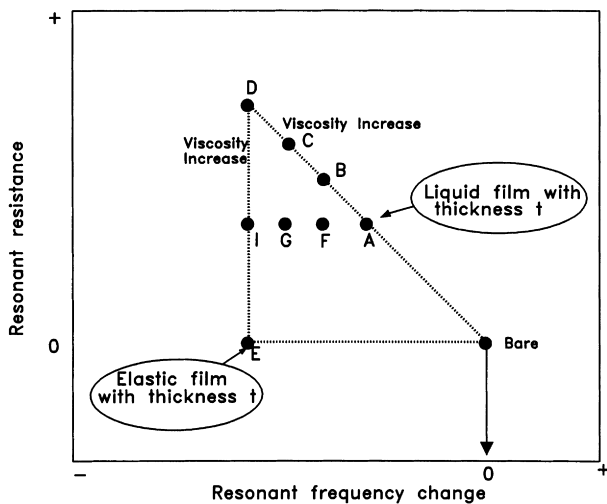


Fig. 4. Quantitative patterns for the changes of resonant frequency and resonant resistance.

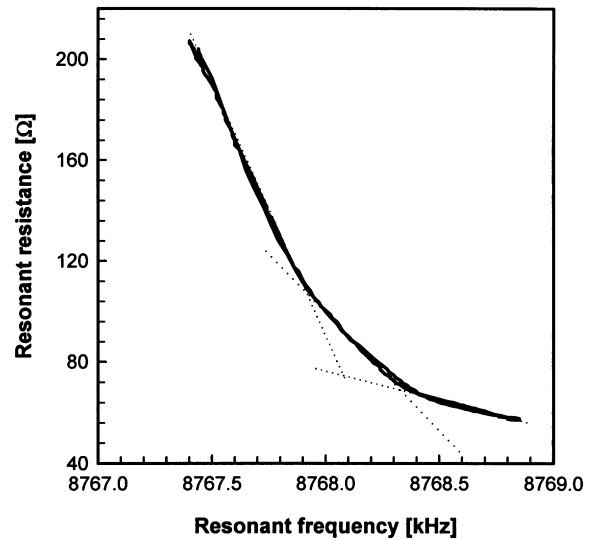


Fig. 5. The  $F-R$  representation of Fig. 3.

resonant resistance is clearer than the response of resonant frequency, and the gap between the heating and cooling curve is smaller than that of the resonant frequency. However, the boundary temperatures are not clearly obtainable using only one of the indexes. The  $F-R$  representation was considered based on our previous work [21].

Fig. 4 shows a  $F-R$  diagram model in contact with air. In Fig. 4, the black dots show quantitative patterns that present the changes of rough viscoelasticity in the viscoelastic film by comparing them with the frequency shift. In Fig. 4,  $A \rightarrow B \rightarrow C \rightarrow D$  shows the path of the increasing viscosity in the fluid film,  $A \rightarrow F \rightarrow G \rightarrow I$  shows the path of the increasing elasticity in the viscous film,  $E \rightarrow I \rightarrow D$  shows the path of the increasing viscosity in the elastic film. More information is available in our original paper described above [21].

In Fig. 5, the  $F-R$  representation from Fig. 3 shows viscosity increasing in the coated film with decreasing frequency and presents three different slopes in the measured temperature range. Intersection points of these slopes are

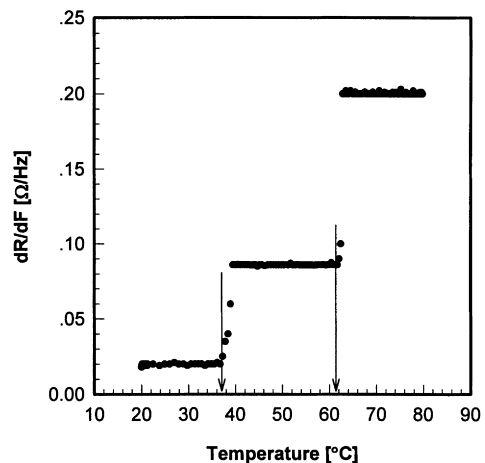


Fig. 6. The detection of phase transition temperature of PMMA/PVAc (50/50) blend film using the relation between  $dR/dF$  and temperature.

clearly obtained as the phase transition points. The first intersection point, meaning the first phase transition, is detectable at the resonant frequency of about 8768.5 kHz and at the resonant resistance of 60 for heating run. The second inflection point is located at the resonant frequency of about 8767.9 kHz and at the resonant resistance of 105.

The  $F$ - $R$  method well describes the relationship between resonant frequency and resonant resistance, but it also shows a difficulty in detecting the phase transition temperature directly. For clearer detection of the phase transition temperature, the relation between  $dR/dF$  and temperature is provided in Fig. 6. To obtain these data, numerical methods (interpolation and differential calculus) were applied to the data in Fig. 5. Physically, the value of  $dR/dF$  means

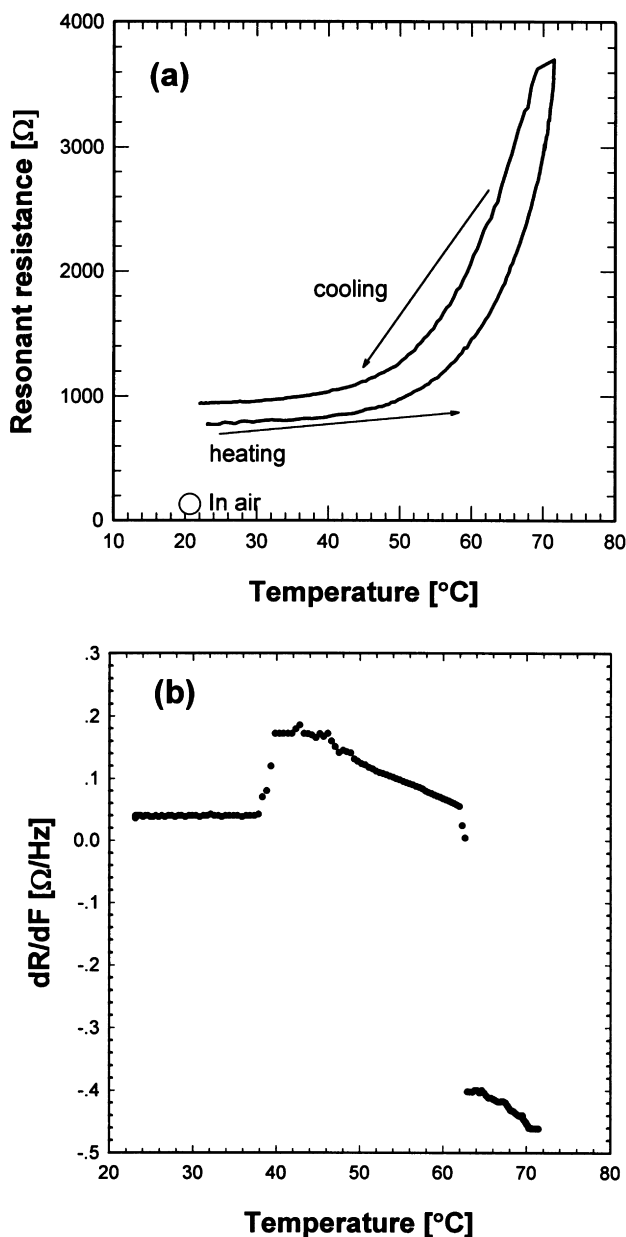


Fig. 7. The resonant resistance (a) and  $dR/dF$  (b) responses of PMMA/PVAc (50/50) blend film-coated quartz crystal immersed in water.

the energy dissipation factor or viscoelasticity factor in the coated film.

In Fig. 6, the values of  $dR/dF$  show almost horizontal lines in the given temperature range, except two non-continuous inflection points. These points indicate the phase transitions of the film. As a result, the phase transition temperatures are 37 and 62°C.

The mechanical property of a blend film at phase transition temperature was also examined by immersing the film-coated quartz crystal in water. Fig. 7 shows the response of resonant resistance (a) for PMMA/PVAc (50/50) blend film-coated quartz crystal in a thermal cycle when it is immersed in water. Because the density and viscosity of the contacted water influence the properties of the film on the quartz crystal, usually, the change of the resonant resistance shows an expanded view from that in air. In Fig. 7(a), the first inflection point is not clearly detectable at the temperature of 37°C and the second phase transition temperature is detectable corresponding to the temperature in Fig. 3.

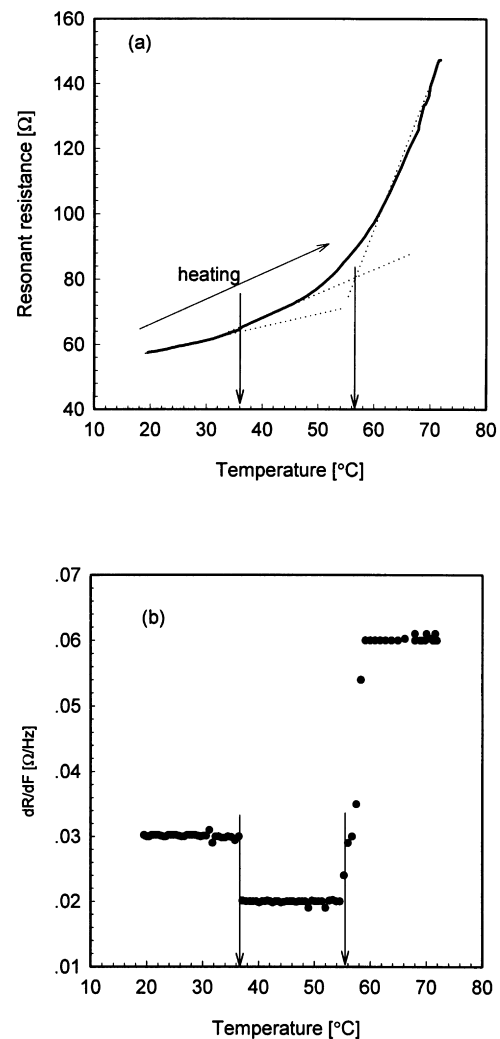


Fig. 8. The responses of resonant resistance (a) and resonant frequency (b) of PMMA/PVAc (50/50) blend film-coated quartz crystal when the lower molecular weight of PMMA is used as a blend component.

Table 1  
Comparison of phase transition temperature between the QCR and DSC methods

	QCR (°C)	DSC (°C)
PVAc	35	35
10/90 (PMMA/PVAc)	39, 67	–
20/80 (PMMA/PVAc)	36, 67	–
30/70 (PMMA/PVAc)	38, 67	38, 70
40/60 (PMMA/PVAc)	38, 64	–
50/50 (PMMA/PVAc)	37, 62	35, 80
60/40 (PMMA/PVAc)	36, 63	–
70/30 (PMMA/PVAc)	37, 65	39, 72
80/20 (PMMA/PVAc)	39, 69	–
90/10 (PMMA/PVAc)	40, 69	–
PMMA	98	100

However, in this figure, the starting value of resonant resistance is not perfectly recovered when the temperature is reassigned to its starting temperature. Fig. 7(b) enables easy detection of phase transition temperatures. In Fig. 7(b), the values of  $dR/dF$  do not show horizontal lines above 45°C and show negative values after the second phase transition temperature. The decreases of the  $dR/dF$  value above 45°C are interpreted to be due to the fact that the polymer blend film is not permeable, i.e. the film has a glassy structure before the first phase transition, but it is diffusible to water above the first transition temperature by the change of morphology, crystalline structure, surface tension of the film and the change of the molecular dynamics of the water. The minus value of the  $dR/dF$  is explained by the oscillation properties, which are influenced by several physical properties of coated films. In the future, we will report on the effects of these properties, such as, the effect of hydrophobic and hydrophilic film coatings on the resonant properties.

Table 1 shows the comparisons of the glass transition

temperatures that are obtained by DSC thermograms and QCR method in the air. The comparison of the QCR data and the DSC data suggests that the transition temperatures from the QCR basically correspond to the results by DSC and are indicative of the phase transition or glass transition temperatures. Each transition point of the blend films corresponds to the phase transition temperatures for the PVAc and the PMMA components. However, it should be noted that there are noticeable differences in the sense of absolute values. Careful inspection of Table 1 indicates that the differences are much larger for the PMMA than the PVAc component in the blend films. The phase transition temperatures of the PMMA component in the blend films measured by the quartz crystal are always lower than those of the DSC results. The discrepancy between the DSC and the quartz crystal method may result from the effect of the thin film of the samples on the quartz crystal compared with that of the DSC. The report done by Mayes shows that the near-surface region of glassy polymers in coatings or thin film exhibits a significant depression in the glass transition temperature due to the chain-end enrichment [22]. Since the thin films are used in the QCR method (thickness about: 0.1  $\mu\text{m}$ ), the results in Table 1 may be related to the surface effect-dependent glass transition temperature and the accuracy for detecting the phase transition temperature is not perfectly comparable in these two methods.

The most interesting fact from the results of the QCR method is that the distances between the two phase transition temperatures are nearer when the blend ratio is higher, i.e. the blend ratios of (40/60), (50/50) and (60/40). But these results do not correspond with the results of the DSC method. We believe this is also reasoned by the thin film nature of the quartz crystal but further investigation is in progress.

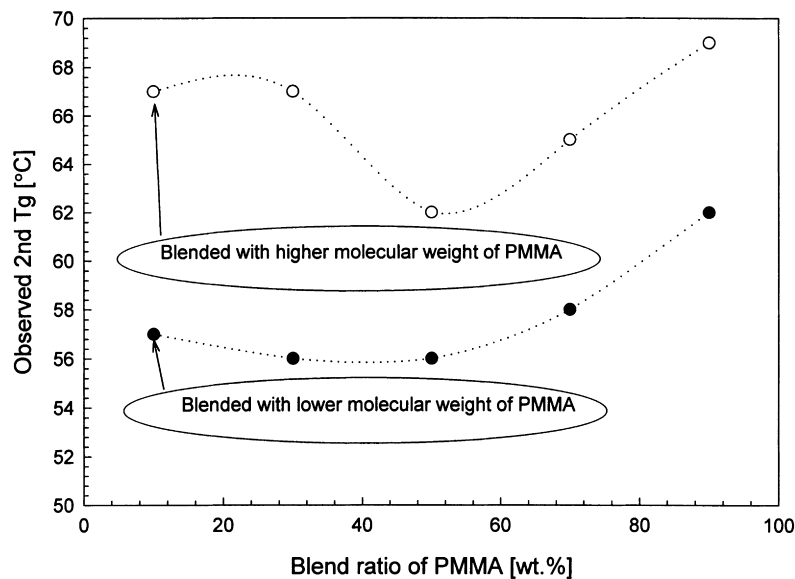


Fig. 9. The phase transition temperatures of PMMA films of lower (○) and higher (●) molecular weight obtained by the QCR method.

### 3.2. Influence of molecular weight on the rheological property

The rheological property changes due to the change of molecular weight in blend films were examined. Fig. 8 shows the results of resonant resistance (a) and  $dR/dF$  (b) in the thermal cycle where the lower molecular weight of the PMMA is used for 50/50 (PMMA/PVAc) blend film. Because the chain length of polymers influences the phase transition properties, the rheological property change of this blend film shows a certain difference compared with when that of a higher molecular weight is used as a blend component. Though Fig. 8(a) indicates the phase transition temperatures, the detailed rheological difference compared with Fig. 3(b) is not clearly

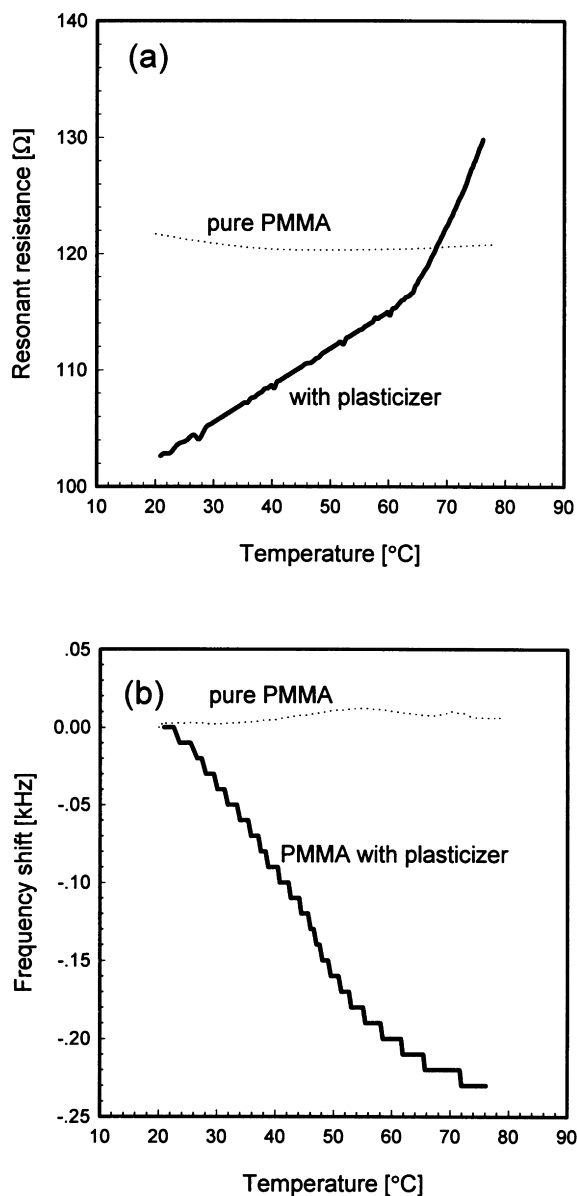


Fig. 10. The resonant resistance (a) and resonant frequency (b) responses of PMMA homopolymer when 2.5 wt% of a plasticizer is included in the film.

understandable. Fig. 8(b) shows obvious differences with the graph of Fig. 6. In Fig. 8(b), the dissipation factors are smallest in the temperature range of 36–56°C, that is after the first phase transition temperature. This is understood to be because the blended molecular length of the PMMA component is about 1/6 of the PMMA component in Fig. 6. Then the PVAc, which is the component of the first phase transition in Fig. 8, is more easily movable through the blend film than when that of the higher molecular weight of the PMMA component is blended. This enhancement of movability in the blend film may allow rearrangement of blend structure.

Fig. 9 shows the comparison of the second phase transition temperature with the different molecular weights of PMMA components for the several blend ratios. When the lower molecular weight of PMMA is used as the blend component, the second phase transition temperatures of the PMMA component are always lower than that of the higher molecular weight of PMMA. The difference of the second phase transition temperatures becomes larger when the ratio of PMMA component is low in the blend films, i.e. the blend ratios of 10/90, 30/70 (PMMA/PVAc). This fact is also understood as a role of the first phase-transited PVAc component, such as, mobility in blend film. In this experiment, we confirmed the possibility that detecting the rheological property changes depended on the molecular size, therefore, it is believed to show the possibility of revealing the unsolved problem in the blend-film rheology, which is the effect of dispersed phase on the second glass transition temperature.

### 3.3. Phase transition of a plasticizer-included PMMA homopolymer

The rheological property of a plasticizer-included PMMA

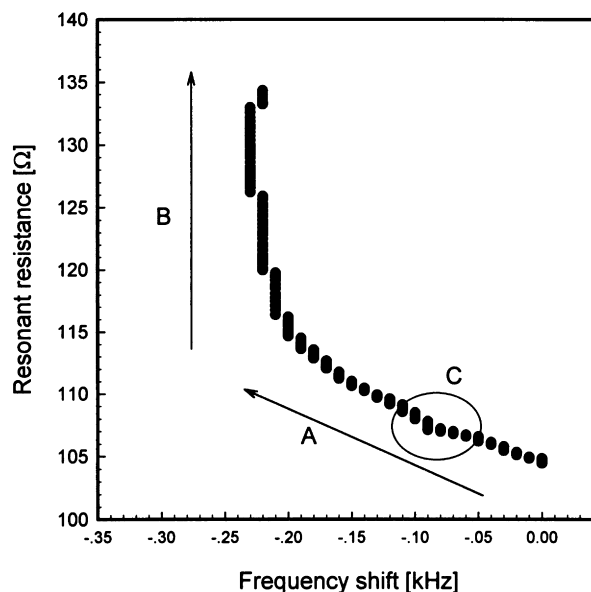


Fig. 11. The  $F$ - $R$  representation of Fig. 10.

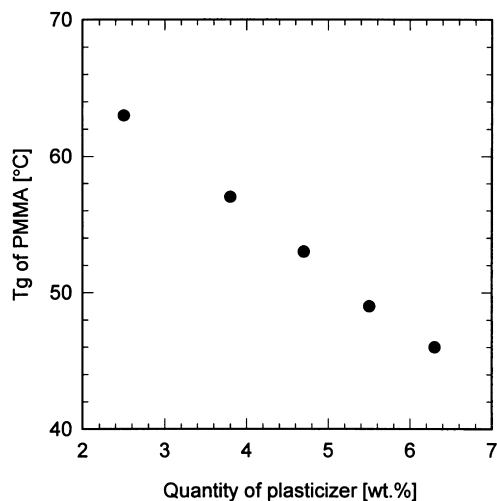


Fig. 12. The phase transition temperatures of PMMA films as a function of the quantity of a plasticizer.

homopolymer film was also investigated using the QCR method.

Fig. 10 shows resonant resistance (a) and resonant frequency (b) responses for a 2.5 wt% plasticizer included PMMA homopolymer film in the second heating run. The results of the PMMA homopolymer, which does not include plasticizer, are also plotted as dashed lines for comparison. In Fig. 10, the influence of plasticizer on the rheological property change in the thermal sweep is clearly shown. In the temperature range examined, the plasticizer free PMMA homopolymer behaves as an elastic film because it shows no inflection part caused by the changes of film property. The resonant resistance of the PMMA film with 2.5 wt% plasticizer increases with increasing temperature and shows an inflection point, meaning the break of its solid state, at 63°C. The response of resonant frequency shows the slope changes at 45 and 58°C on heating but is not clearly understandable.

As shown in Fig. 5, the  $F-R$  method is helpful for clear detection. In the  $F-R$  diagram (Fig. 11) of Fig. 10, clear two slopes exist in the heating run. The increase of the resonant resistance ranging frequency from 8754.82 to 8654.6 kHz, which is denoted as region A in the figure, shows that both viscosity and elasticity increase in the film. After this region, the resonant resistance increases rapidly with small change of resonant frequency at region B, which means only the viscosity factor is increasing in this region. In Fig. 11, there is a questionable region named region C. Region C might be produced by a noise because the slopes before this region and after this region are almost equal, and the frequency shift at this sample is quite small compared with other samples.

The concentration of the plasticizer dependence on the phase transition temperature was investigated using the concentration 2.5–6.3 wt% for the total PMMA film weight. Fig. 12 shows the phase transition temperatures of the

PMMA films with respect to the concentrations of plasticizer in the PMMA homopolymer films. This result was obtained from the relation between the  $dR/dF$  and temperature for second heating runs. The phase transition temperatures of the plasticizer including polymer show a linear relationship with the plasticizer quantity in the concentration range investigated.

#### 4. Conclusions

In this paper, we presented the usability of the QCR in the detection of phase transition temperature and microrheological property changes of thin polymer films. The results of the QCR method for detecting glass transition temperature showed a correspondence with that of the DSC but small difference was observed because of the surface effect of the thin films. The  $F-R$  method and the correlation between the  $dR/dF$  and temperature enabled the clearer detection of phase transition temperature. The plasticizer-included PMMA films showed the decrease of glass transition temperature due to the added plasticizer quantity was linear. As a consequence, the QCR methodology was well applied to the detection of rheological property changes of the thin films.

#### Acknowledgements

Kim J.M. gratefully acknowledges the support for research carried out by the Korea Science and Engineering Foundation (KOSEF) and Advanced Technology Center of Seiko Instruments, Inc.

#### References

- [1] Sauerbrey GZ. *Physik* 1959;155:206.
- [2] Nomura T, Minemura A. *Nippon Kagaku Kaishi* 1980;1980:1621.
- [3] Kanazawa KK, Gordon JG. *Anal Chim Acta* 1985;177:99.
- [4] Lasky SJ, Buttry DAJ. *Am Chem Soc* 1988;110:6258.
- [5] Thompson M, Arthur CL, Dhaliwal GK. *Anal Chem* 1986;58:1206.
- [6] Richard CE, Michael DW. *J Am Chem Soc* 1988;110:8623.
- [7] Bruckenstein S, Swathirajan S. *J Electroanal Chem* 1985;30:851.
- [8] Schumacher R, Borges G, Kanazawa KK. *Surf Sci* 1985;163:L621.
- [9] Muramatsu H, Tamiya E, Karube I. *Anal Chem* 1988;60:2142.
- [10] Borjas R, Buttry DA. *J Electroanal Chem Interfacial Electrochem* 1990;280:73.
- [11] Muramatsu H, Ye X, Suda M, Sakuhara T, Ataka T. *J Electroanal Chem* 1992;322:311.
- [12] Kelly AJ, Oyama N. *J Phys Chem* 1991;95:95.
- [13] Muramatsu H, Ye X, Ataka T. *J Electroanal Chem* 1993;347:247.
- [14] Nielsen LEJ. *Am Chem Soc* 1995;75:1435.
- [15] Nishi T, Wang T. *Macromolecules* 1975;8 (6):909.
- [16] Griffiths MD, Maisey LJ. *Polymer* 1976;17:869.
- [17] Michael R, Fredrick H, Bongt K. *Anal Chem* 1996;68:2219.
- [18] Muramatsu H, Egawa A, Ataka K. *J Electroanal Chem* 1995;388:89.
- [19] Zhou T, Nie L, Ya S. *J Electroanal Chem* 1990;293:1.
- [20] Chang SM, Kim JM, Muramatsu H, Ataka T, Cho WJ, Ha CS. *Polymer* 1996;37 (16):3757.
- [21] Muramatsu H, Kimura K. *Anal Chem* 1992;64:2502.
- [22] Mayes AM. *Macromolecules* 1994;27:3114.